Research in Astron. Astrophys. **2011** Vol. **11** No. **7**, 776–786
http://www.raa-journal.org *http://www.iop.org/journals/raa*

Research in Astronomy and Astrophysics

Combining optical and X-ray observations of galaxy clusters to constrain cosmological parameters *

Heng Yu and Zong-Hong Zhu

Department of Astronomy, Beijing Normal University, Beijing 100875, China; *zhuzh@bnu.edu.cn*

Received 2010 October 12; accepted 2011 March 18

Abstract Galaxy clusters present unique advantages for cosmological study. Here we collect a new sample of 10 lensing galaxy clusters with X-ray observations to constrain cosmological parameters. The redshifts of the lensing clusters lie between 0.1 and 0.6, and the redshift range of their arcs is from 0.4 to 4.9. These clusters are selected carefully from strong gravitational lensing systems which have both X-ray satellite observations and optical giant luminous arcs with known redshifts. Giant arcs usually appear in the central region of clusters, where mass can be traced with luminosity quite well. Based on gravitational lensing theory and a cluster mass distribution model, we can derive a ratio using two angular diameter distances. One is the distance between lensing sources and the other is that between the deflector and the source. Since angular diameter distance relies heavily on cosmological geometry, we can use these ratios to constrain cosmological models. Moreover, X-ray gas fractions of galaxy clusters can also be a cosmological probe. Because there are a dozen parameters to be fitted, we introduce a new analytic algorithm, Powell's UOBYQA (Unconstrained Optimization By Quadratic Approximation), to accelerate our calculation. Our result demonstrates that this algorithm is an effective fitting method for such a continuous multi-parameter constraint. We find an interesting fact that these two approaches are separately sensitive to Ω_Λ and Ω_M. By combining them, we can get reasonable fitting values of basic cosmological parameters: $\Omega_\mathrm{M} = 0.26^{+0.04}_{-0.04}$, and $\Omega_\Lambda = 0.82^{+0.14}_{-0.16}$.

Key words: X-rays: galaxies: clusters — gravitational lensing — cosmological parameters

1 INTRODUCTION

Cosmic acceleration expansion was initially discovered from supernovae observations (Riess et al. 1998; Perlmutter et al. 1999). Then, the cosmic microwave background (CMB) anisotropy power spectrum (Spergel et al. 2003) confirmed that our universe is almost flat and that the density of matter is relatively low. Such conclusions have subsequently been supported by more precise supernova data (Riess et al. 2004; Davis et al. 2007; Kowalski et al. 2008) and CMB observations (Spergel et al. 2007; Komatsu et al. 2009).

∗ Supported by the National Natural Science Foundation of China.

Furthermore, many other independent works, such as the light element abundance from Big Bang Nucleosynthesis (Burles et al. 2001), the baryon acoustic oscillations (BAO) detected in the SDSS sky survey (Eisenstein et al. 2005), radio galaxies (Daly et al. 2009) and gamma-ray bursts (Amati et al. 2008), etc., all give consistent results. If there is a component with negative pressure filling our universe, dubbed dark energy, then such acceleration can be explained within an existing theoretical framework. Various models have been proposed to explain dark energy, such as typical dynamical scalar field quintessence (Caldwell et al. 1998), phantom corrections (Caldwell 2002), a joint quintom scenario (Feng et al. 2005) and chaplygin gas (Zhu 2004; Gorini et al. 2005; Zhang & Zhu 2006), etc. In addition, there are still many other astronomers who doubt the existence of such a strange material. They are trying to find another way to understand this accelerating universe. Modified Newtonian dynamics (MOND, Milgrom 2001), the Modified Friedmann Equation (Freese & Lewis 2002; Zhu et al. 2004b), the Dvali-Gabadadze-Porrati Mechanism (DGP, Dvali et al. 2000) and so on are all such attempts. However, until now none of these models have presented overwhelming advantages. We need more observational evidence. In addition to updating the precision of current data, we are also searching for new potential probes, for example, galaxy clusters.

Galaxy clusters, as the largest dynamic systems known in the universe, retain a deep imprint of the big bang. Their correlation function provides direct measurement of the matter distribution power spectrum. The BAO peak has already been found for luminous red galaxies (Eisenstein et al. 2005). When there are enough galaxy clusters, we can perform the same measurement at a much larger scale (Borgani & Guzzo 2001) and their mass distributions at different redshifts can be described by the Press-Schechter function (Press & Schechter 1974). This relation reflects the linear growth rate of density perturbations. With such connection, clusters can provide constraints on matter and dark energy densities (Borgani et al. 1999; Vikhlinin et al. 2009). Hot gases of galaxy clusters also interact with cosmic microwave background photons and distort their spectrum. Such phenomenon is called the Sunyaev-Zel'dovich effect (SZ effect for short, Sunyaev & Zeldovich 1972). Combining this effect with the observations of corresponding clusters' X-ray luminosity, we can measure the Hubble constant for a certain cosmology or give a rough estimate of cosmological parameters (Mason et al. 2001; Reese et al. 2002; Schmidt et al. 2004; Zhu & Fujimoto 2004; Jones et al. 2005; Bonamente et al. 2006). There have already been many attempts to combine multiple observations of galaxy clusters to study dark energy (Molnar et al. 2004; Majumdar & Mohr 2004; Cacciato et al. 2009; Oguri & Takada 2011). For more detailed reviews we suggest Rosati et al. (2002), Voit (2005) and Borgani (2006).

The two methods adopted here are based on the physical structure and properties of individual clusters. They can give a good estimate of cosmological parameters, as we will see. The first one comes from strong lensing arcs. From X-ray luminosity and temperature, we can model the mass distribution of a cluster. Giant arcs generated by the highly concentrated gravity of a galaxy cluster are perfect indicators of its projected surface mass density. Then we can derive an observational value to constrain cosmological models. This method was first used by Sereno (2002) and improved in Sereno & Longo (2004). We collect a new data set from literature and the online database BAX. Several effective criteria are introduced to rule out improper clusters. There are 10 clusters selected to make up a new sample. This new set can give more reasonable results compared with the last one supplied by Sereno & Longo (2004). We will discuss it in detail in Section 2. The second way is based on the assumption of constant X-ray gas mass fraction. This method was developed by Allen et al. (2001, 2004, 2008) and has been proven to be effective. Due to the complex physical mechanism involved, there are many parameters to fit. To search multi-parameter space more effectively, we introduce a new optimization algorithm UOBYQA (Unconstrained Optimization By Quadratic Approximation) (Powell 2002) to marginalize external parameters. This algorithm has been widely accepted in the field of mathematics. This should be its first application in cosmology. The algorithm is summarized in Section 3. The combined analysis and discussions are presented in the last section.

2 LENSING CLUSTER

2.1 Theoretical Foundation

Gravitational lensing is a successful prediction of general relativity. After it was confirmed by quasar observation in 1979 (Walsh et al. 1979), Paczynski & Gorski (1981) tried to use lensing images as indicators to estimate cluster mass and constrain cosmological constants. However, it is very difficult to find the deflectors in lensing cases of point-like sources, so this approach was seldom used until recent years (Futamase & Yoshida 2001). Later, giant arcs around galaxy clusters were discovered in clusters A370 and Cl2224 (Lynds & Petrosian 1986). They can also be used to constrain clusters' projected mass, since clusters are easy to observe. Breimer & Sanders (1992) did pioneering work. They estimated the virial mass of cluster A370 with nearly 30 member galaxies' velocities, then compared with the lensing condition and obtained an original estimate of cosmological parameters. However, member galaxies are discrete and the velocity dispersion of distant objects is usually hard to obtain. Subsequently, Sereno & Longo (2004) used continuous X-ray luminosity instead. When a galaxy cluster is relaxed enough, the pressure of its hot gas can balance its self-gravity. In this case, we can use a hydrostatic isothermal spherically symmetric β-model (Cavaliere & Fusco-Femiano 1976) to describe the intracluster medium (ICM) density profile

$$n_{\rm e}(r) = n_{\rm e0}\left(1 + r^2/r_{\rm c}^2\right)^{-3\beta_{\rm X}/2}, \tag{1}$$

where $n_{\rm e0}$ is the central electron density, $\beta_{\rm X}$ describes the slope and $r_{\rm c}$ stands for the core radius. Assuming all the gases have the same emissivity of hot bremsstrahlung radiation, in other words, isothermal (with the temperature $T_{\rm X}$), the gravity of a relaxed cluster and its gas pressure should balance each other according to the hydrostatic equilibrium condition. With the approximation of spherical symmetry we can estimate mass distribution with gas density, which comes from the luminosity fitting result. The cluster's mass profile can be given in the form

$$M(r) = \frac{3k_{\rm B}T_{\rm X}\beta_{\rm X}}{G\mu m_{\rm p}}\frac{r^3}{r_{\rm c}^2 + r^2}, \tag{2}$$

where $k_{\rm B}$ is the Boltzmann constant, $m_{\rm p}$ is the proton mass and μ is the mean molecular weight, which is usually 0.6 (Rosati et al. 2002). Then we can obtain the projected surface mass density. Combining the result with the critical surface mass density of lensing arcs (Schneider et al. 1992), an independent Hubble constant ratio can be expressed by several observational parameters

$$\frac{D_{\rm ds}}{D_{\rm s}}\Big|_{\rm obs} = \frac{\mu m_{\rm p}c^2}{6\pi}\frac{1}{k_{\rm B}T_{\rm X}\beta_{\rm X}}\sqrt{\theta_{\rm t}^2 + \theta_{\rm c}^2}, \tag{3}$$

where $T_{\rm X}$, $\beta_{\rm X}$ and $\theta_{\rm c}$ all come from the X-ray data fitting. Here the θ terms are dimensionless angular variables, the radius divided by angular diameter distance to the cluster ($r/D_{\rm d}$). Under a flat Friedman-Walker metric, the angular diameter distance between an observer at $z_{\rm d}$ and a source at $z_{\rm s}$ is not equal to $D_{\rm s} - D_{\rm d}$. It should be integrated from $z_{\rm d}$ to $z_{\rm s}$ as

$$D_{\rm ds} = \frac{c}{H_0(1 + z_{\rm s})}\int_{z_{\rm d}}^{z_{\rm s}}\frac{dz}{E(z)}. \tag{4}$$

The position of tangential critical curve $\theta_{\rm t}$ is usually deemed equal to observed arc position $\theta_{\rm arc}$. Considering the deviation of the extended lensing source position, the deflection angle is slightly different from the arc radius angle, $\theta_{\rm t} = \epsilon\theta_{\rm arc}$. The correction factor is $\epsilon = (1/\sqrt{1.2}) \pm 0.04$ (Ono et al. 1999). Then the χ^2 test can be carried out between observational data and theoretical models.

2.2 Data Selection

The number of clusters with arcs is still very limited and just a small fraction of these arcs have known redshifts. At first, we refer to the sample of Sand et al. (2005) to look for arcs with redshifts. Their catalog contains 104 tangential arcs from 128 clusters, but only 58 arcs from 27 clusters have redshift values. When there are several arcs from the same source (with the same redshift), we prefer to select the farthest one in general. Because strong lensing arcs usually happen in the very central part of galaxy clusters, giant arcs are always close to the cores of clusters. In addition, the beta model brightness profile usually has better fitting results in outskirts. Therefore, we choose the farthest part in order to avoid possible substructures and to decrease the fitting deviation from the β model. In this case, arc H5b (26.3 arcsec) of A2390 is adopted instead of H5a (20.7 arcsec). For arcs from different sources around one cluster, we treat them as independent events. They will all be adopted as long as they can satisfy the criteria given below.

In the second stage, redshifts and temperatures of these galaxy clusters can be found directly from on-line databases, such as CDS (the Strasbourg Astronomical Data Center) or NED (the NASA/IPAC Extragalactic Database), with their full name. Here we choose a new database established especially for X-ray galaxy clusters – BAX[1]. It provides detailed information about clusters. Following referred literature given by BAX, we can get fitting parameters β and $\theta_{\rm c}$. To minimize systematic error caused by different work and systems, it is better to limit data sources within a few articles. In this paper, we use the fitting result of Chandra (Bonamente et al. 2006). For the clusters not presented by that paper, we refer to the catalog[2] of Ota & Mitsuda (2004), which is based on the observations of the ROSAT and ASCA satellites. The clusters inherited from Sereno & Longo (2004) are all updated in this way.

Table 1 Sample of Lensing Galaxy Clusters with X-ray Observations

Cluster	Arc	$z_{\rm d}$	$z_{\rm arc}$	$\theta_{\rm arc}('')$	$k_{\rm B}T_{\rm X}({\rm keV})$	$\beta_{\rm X}$	$\theta_{\rm c}('')$	ρ/ρ_0	Ref
3C220.1	A1	0.61	1.49	8.6	5.56±1.38	0.84±0.45	8.1±4.2	29219	[1]
Abell 2390	H5b	0.228	4.05	26.3	9.35±0.15	0.46±0.01	12.1±1.4	59463	[1]
Abell 2667	A1	0.226	1.034	14.7	6.15±0.61	0.52±0.01	13.4±0.8	65462	[1]
MS 0451.6–0305	A1	0.550	2.91	31.8	10.4±0.7	0.767±0.018	33.5±1.2	4177	[2]
MS 1512.4	cB58	0.372	2.72	5.1	3.39±0.4	0.54±0.06	8.3±2.4	52805	[1]
MS 2137.3–2353	A01	0.313	1.501	15.5	4.96±0.11	0.6±0.04	8.3±1.5	38603	[1]
PKS 0745–191	A	0.103	0.433	19.2	7.97±0.28	0.52±0.01	16.4±0.9	271090	[1]
Abell 68	C0c	0.255	1.6	8.0	10.0±1.1	0.721±0.035	49.6±3.6	17867	[2]
CL0024.0	E	0.391	1.675	4.0	4.38±0.27	0.41±0.03	11.1±4.1	31586	[1]
MS 2053.7	AB	0.583	3.146	15.1	4.7±0.5	0.639±0.033	15.3±1.6	6324	[2]

Notes: Reference [1] Ota & Mitsuda (2004) and [2] Bonamente et al. (2006).

Then we collect about 20 clusters with all necessary parameters. However, not all of them are approximately isothermal, spherically symmetric or even in hydrostatic equilibrium. We must check them carefully to eliminate the arcs generated by unrelaxed clusters (Smith et al. 2003).

2.3 Criteria

A static cluster should have regular morphology both in the optical and X-ray bands. In the optical band, they usually present spatial symmetry and have a regular shape. In the X-ray band, sharp

[1] BAX: *http://bax.ast.obs-mip.fr/*, other databases such as Simbad, NED, etc., only accept clusters' full name like RXJ1347.5–1145. The abbreviations listed here are only for convenience and cannot be used to search directly.

[2] Ota's catalog was not contained in the article, but was put on her own website.

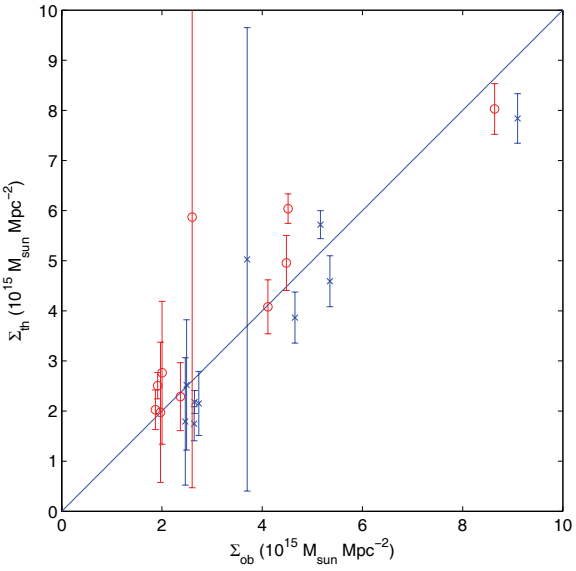

Fig. 1 Relationship between lensing surface mass density ($M_\odot$ Mpc^{-2}) and projected surface density from the X-ray model. Asterisks come from the standard model ($\Omega_\mathrm{M} = 0.3$, $\Omega_\Lambda = 0.7$); Circles are calculated under $\Omega_\mathrm{M} = 0$, $\Omega_\Lambda = 1$.

central surface brightness and regular elliptical isophotes are both common characteristics of dynamically relaxed clusters. However, such descriptions rely heavily on the resolution of equipment. We need more concrete standards.

Weak gravitational lensing was used to test X-ray mass distributions many years ago. Mahdavi et al. (2008) confirm that they are consistent with each other at the inner part. Although he used the Navarro-Frenk-White (NFW) dark matter halo model (Navarro et al. 1996), the results ensure that hydrostatic equilibrium is applicable within radius r_{2500} (which means the mean mass density is 2500 times the universe's critical density at that redshift). We can find from Table 1 that all our arcs lie deep inside this region. To avoid a possible large disagreement with the inner mass estimation, we also compare lensing mass with theoretical predictions to check our mass model. According to the strong lensing equation of an isothermal sphere, the projected mass is

$$\Sigma_\mathrm{ob} = \frac{c^2}{4\pi G}\frac{D_\mathrm{s}}{D_\mathrm{d}D_\mathrm{ds}}\sqrt{\frac{\theta_\mathrm{t}^2}{\theta_\mathrm{c}^2}+1}. \tag{5}$$

From Equation (2), we can derive a typical theoretical surface density, which is

$$\Sigma_\mathrm{th} = \frac{3}{2G\mu m_\mathrm{p}}\frac{k_\mathrm{B}T_\mathrm{X}\beta_\mathrm{X}}{\theta_\mathrm{c}}\frac{1}{D_\mathrm{d}}. \tag{6}$$

Mass values from the above two equations should be consistent with each other for a spherically relaxed cluster, as shown in Figure 1. Because this test is not model independent, we do not take it as a selection tool, but just use it to examine the data with the best fit model.

In Equation (4), the distance between lens and sources (integrated from z_d to z_s) should always be smaller than that between the arc sources and the observer (integrated from 0 to z_s), although the angular distance does not monotonically ascend with redshift. So these clusters should satisfy:

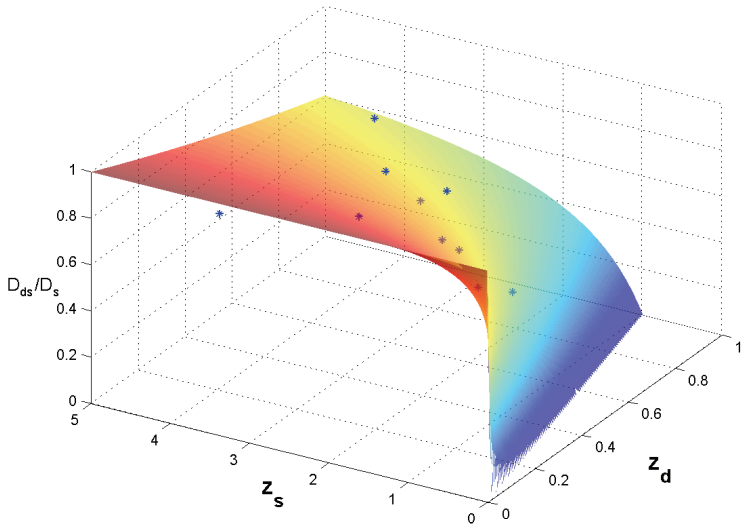

Fig. 2 3-D Hubble diagram distribution of the sample galaxy clusters. Here X axis is the redshift of the deflectors, Y is that of the arc and Z is the second criterium $D_{\rm ds}/D_{\rm s}$. The reference surface comes from our best-fit model below. The intersecting line between the fitted surface and the bottom of the box is $z_{\rm d} = z_{\rm s}$. The jagged edge is merely caused by our program.

$D_{\rm ds}/D_{\rm s}|_{\rm obs} < 1$. In Figure 2 we can see this more clearly. The points above the box indicate that the corresponding clusters are not self-consistent. They need more precise descriptions for cosmological tests. Unfortunately, this condition rules out half of the selected lensing arcs.

We also discard the arcs whose positions are too far from the characteristic radius ($\theta_{\rm arc} > 3\theta_{\rm c}$). Such a cluster has a relatively small core radius and a much bigger arc radius. In this case, the X-ray observations cannot trace matter in the regions where lensing arcs exist. The extrapolation results of the model for the inner region are no longer reliable. They may greatly influence the constraint result. For example, the most luminous cluster in the sky, RXJ1347, is still undergoing a merging process (Allen et al. 2004; Ota et al. 2008). It will cause a really serious deviation when counted in. In fact, it is responsible for the high Ω_Λ value (about 1) in the paper of Sereno & Longo (2004). This may also explain the systematic bias in the articles of Breimer & Sanders (1992) and Sereno (2002). A similar situation also happens to the C arc (38.1 arcsec) of A2390. Hence, only an inner arc H5b is adopted.

Finally, we obtain the sample of 10 clusters listed in Table 1. The redshifts of these clusters range from 0.1 to 0.6, and the farthest arc is H5b of A2390 $z = 4.05$. All of these arcs appear in the very central region. The average surface density within the arcs is listed in the n column with the unit of the critical universe density at the corresponding redshift. Data for cosmological fitting are shown in Table 2. Errors are calculated with the error propagation equation.

3 X-RAY GAS MASS FRACTION

There is another way to connect the physical characteristics of galaxy clusters to cosmological parameters. As mentioned above, in hydrostatic equilibrium both the X-ray gas mass distribution and the total mass profile which balances it can be derived from the surface brightness profile (White & Frenk 1991). Because of the large scale of the clusters, their matter content can be taken as a fair

Table 2 Values of $D_{\rm ds}/D_{\rm s}$ from Equation (3)

Cluster	$D_{\rm ds}/D_{\rm s}$	$\sigma(D_{\rm ds}/D_{\rm s})$
3C220.1	0.341	0.359
A2390	0.737	0.053
A2667	0.837	0.124
MS0451	0.785	0.087
MS1512	0.734	0.330
MS2137	0.778	0.105
PKS0745	0.818	0.065
A68	0.982	0.225
CL0024	0.919	0.430
MS2053	0.968	0.209

sample of the whole Universe (White et al. 1993). The baryonic fraction measurement of clusters can be connected with the geometry. Sasaki (1996) and Pen (1997) first applied this property to a cosmological test. Allen et al. (2001) assumed that the X-ray gas mass fraction within r_{2500} is invariant with redshift. Then the angular distance of clusters can be derived in a different way from that in the reference cosmological model (Allen et al. 2004; Zhu et al. 2004a; Allen et al. 2008). In reference cosmology with $h = H_0/100\ {\rm km\ s^{-1}\ Mpc^{-1}}$, $\Omega_\Lambda = 0.7$ and $\Omega_{\rm m} = 0.3$, we have

$$f_{\rm gas}^{\Lambda{\rm CDM}}(z) = \frac{KA\gamma b(z)}{1+s_z}\frac{\Omega_{\rm b}}{\Omega_{\rm m}}\left[\frac{d_A^{\Lambda{\rm CDM}}(z)}{d_A^{\rm mod}(z)}\right]^{1.5}, \tag{7}$$

where K is a calibration constant, A is equal to $(\theta_{2500}^{\Lambda{\rm CDM}}/\theta_{2500})^\eta$, and γ stands for non-thermal pressure in the clusters; $b(z)$ is the depletion factor with the expression of $b_0(1+\alpha_b z)$; $s(z)$ models the baryonic mass fraction in stars, which can also be expressed as $s_0(1+\alpha_{\rm s} z)$. Two weak priors are also needed here: Hubble parameter $h = 0.72 \pm 0.24$ and mean baryon density $\Omega_{\rm b}h^2 = 0.0214 \pm 0.006$ (Allen et al. 2008).

Obviously, so many parameters are not easy to calculate with common methods. Allen et al. (2008) used the popular MCMC (Markov Chain Monte Carlo) program CosmoMC (Lewis & Bridle 2002). For such a nonlinear and non-derivable function, the stochastic process can generate the right distribution, but it needs a large point set to draw smooth contour lines and obtain precise errors. In fact, we do not need to obtain all parameters' biases at the same time. In our case, we are only concerned with cosmological parameters, so we can just constrain two parameters each time and marginalize the rest. In the actual calculation, we assemble the parameters K, γ, b_0 and $S_0 + 1$ into one factor. Marginalizing them together will not affect our final results. Then we use grids to generate reference points on parameters' phase space. It is easy to calculate contour lines for them. We just need to search for the most optimal value in the space of the rest of the parameters to accomplish marginalization. Considering that all the physical processes are still continuous, and their functions have a definite slope, we attempt a new analytical algorithm – the Powell's "Unconstrained Optimization BY Quadratical Approximation" (UOBYQA) algorithm (Powell 2002). It was developed from a previous linear approximation algorithm (Powell 1994). Briefly, it constructs a quadratic model by Lagrange interpolation to obtain curvatures of the objective function and searches for the nearest optimum with these curvatures. This method is insensitive to noisy surfaces and its calculated quantity will not increase too much with multiple parameters. Here we adopt a ready-made program module CONDOR (COnstrained, Non-linear, Direct, parallel Optimization using the trust Region method for high-computing load function)[3]. This specific module expands Powell's algorithm to the constrained condition by defining active sets for linear constraints and using sequential quadratic

[3] It is available at *http://www.applied-mathematics.net.*

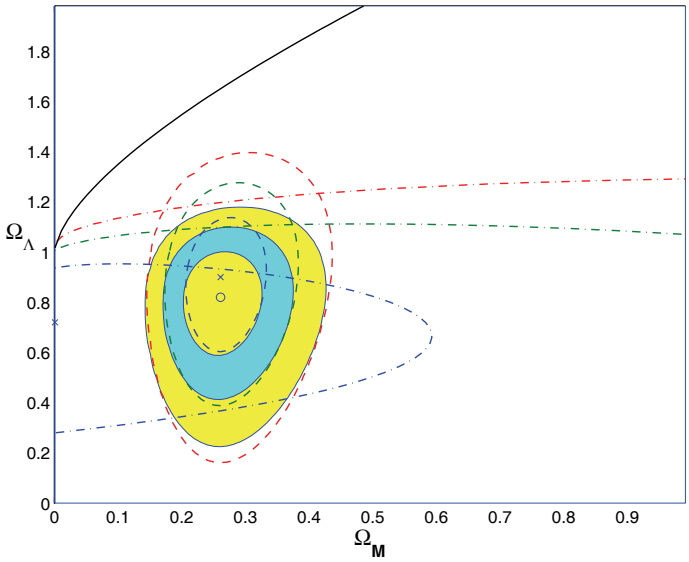

Fig. 3 Dashed line gives the result of X-ray gas mass fraction, while the dash-dotted line comes from the lensing cluster. Two "×" symbols give their best fitting values separately. The shaded regions show the $1\,\sigma$, $2\,\sigma$ and $3\,\sigma$ confidence regions for combining constraints, corresponding to $\Delta\chi^2$ values of 2.30, 6.17, and 11.8. The small inner circle is the best fitting point: $\Omega_{\rm M} = 0.26^{+0.04}_{-0.04}$ and $\Omega_\Lambda = 0.82^{+0.14}_{-0.16}$.

programming to deal with non-linear constraints. It also adds the support of parallel programming to increase efficiency (Frank & Bersini 2005).

With a sample of 42 galaxy clusters (Allen et al. 2008), we run the program several times with different starting points to make sure the result is stable. We do not find any exceptions. The final optimum we obtain, with 68 percent confidence limits, is $\Omega_{\rm M} = 0.26 \pm 0.04$ and $\Omega_\Lambda = 0.9^{+0.14}_{-0.18}$ with minimum $\chi^2 = 41.8$. Contours are shown with dashed lines in Figure 3. This result is very consistent with the result of Allen et al. (2008), which is $\chi^2 = 41.5$, $\Omega_{\rm M} = 0.27 \pm 0.06$ and $\Omega_\Lambda = 0.86 \pm 0.19$.

4 RESULT AND DISCUSSION

Our sample is not big enough to calculate a precise constraint for the equation of state, so we use a simple cosmological model $E(z) = \sqrt{\Omega_{\rm M}(1+z)^3 + \Omega_\Lambda + (1-\Omega_{\rm M}-\Omega_\Lambda)(1+z)^2}$. Because these two methods use a different cluster sample, we fit them separately and sum their χ^2 to get the final fitting results. As can be seen in Figure 3, the dashed lines give the result of X-ray gas mass fraction and the dash-dotted contours come from lensing clusters. The shaded region shows the combined constraint. The small inner circle gives the best fitting values $\Omega_{\rm M} = 0.26^{+0.04}_{-0.04}$ and $\Omega_\Lambda = 0.82^{+0.14}_{-0.16}$ at 68% confidence limits. These results are in agreement with the basic facts we know from other observations.

When combining results from these two methods, we find that these two constraining methods, when separately applied to clusters, are sensitive to different cosmological parameters. Their contour regions are nearly orthogonal. The angular diameter distance ratio estimated from strong lensing arcs sensitively depends on Ω_Λ. The best fitting value is $\Omega_\Lambda = 0.74^{+0.18}_{-0.36}$. It is better than the result from constraining the gas fraction. However, it cannot give any significant constraint for $\Omega_{\rm M}$. In addition,

the gas fraction of clusters is more effective in constraining $\Omega_{\rm M}$. So, when we combine these two methods together, the unified constraint is better than both of them taken separately. Such results are still preliminary. Due to the complexity of clusters themselves, there is still a lot of work to do to improve these methods.

The common radial temperature distribution of clusters makes it difficult to use an isothermal approximation. However, in the small scale within arcs, temperatures will not change dramatically, even for cool-core clusters. The clusters which have substructures or even whose which are experiencing merging cannot be described simply. At least we can rule them out by our criteria. The X-ray observations of our new lensing cluster sample come from three different satellites: ROSAT, ASCA (Ota & Mitsuda 2004) and CHANDRA (Bonamente et al. 2006). The different equipment may also cause systematical errors, which are hard to estimate. Considering that two previous telescopes are comparatively old, fitting results from CHANDRA or XMM may give better results.

These two methods use two different cluster sample sets with some common clusters (A2390, MS2137, etc.). The deviation of different observations may also be indirectly counted. Hence, it is necessary to select a unified set to share the same clusters and observational parameters. The mass profile models used by these methods are different. The strong lensing approach uses the β-model to fit surface brightness, while the gas fraction method uses the NFW model to describe the dark matter halo. As we have seen in Table 1, lensing arcs usually appear in the central region of clusters, where the NFW model can usually give a better fitting result than that of the isothermal sphere model (Comerford et al. 2006; Schmidt & Allen 2007). If we can unify the two methods into the same mass profile model, the results may be more convincing.

Compared with other cosmological observations, our cluster sample is quite small, and its range of redshift is also limited. According to Yamamoto & Futamase (2001), a data set containing more than 20 clusters can more precisely constrain the dark energy equation of state. It will not take long to achieve that goal. There are many giant arc survey projects currently proceeding (Gladders et al. 2003; Hennawi et al. 2008). The number of newly discovered arcs is increasing rapidly. Waiting for results from their redshift measurement is only a matter of time. The next generation of X-ray telescopes, e.g. the International X-ray Observatory (IXO) (White et al. 2010), the extended Roentgen Survey with an Imaging Telescope Array (eRosita) (Predehl et al. 2010) and the Wide Field X-ray Telescope (WFXT) (Murray & WFXT Team 2010), will carry out new surveys more precisely in a much larger field. Future observations will definitely enlarge our known data sets and make these methods more powerful.

Acknowledgements This work was supported by the National Science Foundation of China under the Distinguished Young Scholar Grant 10825313 and by the Ministry of Science and Technology's National Basic Science Program (Project 973) under grant No. 2007CB815401. We are grateful to Zi Xu for her constructive suggestions on optimization algorithms and for introducing the powerful program CONDOR. We also thank Paolo Tozzi, Xiang-Ping Wu and Xing Wu for their helpful comments.

References

Allen, S. W., Ettori, S., & Fabian, A. C. 2001, MNRAS, 324, 877
Allen, S. W., Rapetti, D. A., Schmidt, R. W., et al. 2008, MNRAS, 383, 879
Allen, S. W., Schmidt, R. W., Ebeling, H., Fabian, A. C., & van Speybroeck, L. 2004, MNRAS, 353, 457
Amati, L., Guidorzi, C., Frontera, F., et al. 2008, MNRAS, 391, 577
Bonamente, M., Joy, M. K., LaRoque, S. J., et al. 2006, ApJ, 647, 25
Borgani, S. 2006, arXiv:astro-ph/0605575
Borgani, S. & Guzzo, L. 2001, Nature, 409, 39
Borgani, S., Rosati, P., Tozzi, P., & Norman, C. 1999, ApJ, 517, 40

Breimer, T. G. & Sanders, R. H. 1992, MNRAS, 257, 97
Burles, S., Nollett, K. M., & Turner, M. S. 2001, ApJ, 552, L1
Cacciato, M., van den Bosch, F. C., More, S., et al. 2009, MNRAS, 394, 929
Caldwell, R. R. 2002, Phys. Lett. B, 545, 23
Caldwell, R. R., Dave, R., & Steinhardt, P. J. 1998, Phys. Rev. Lett., 80, 1582
Cavaliere, A. & Fusco-Femiano, R. 1976, A&A, 49, 137
Comerford, J. M., Meneghetti, M., Bartelmann, M., & Schirmer, M. 2006, ApJ, 642, 39
Daly, R. A., Mory, M. P., O'Dea, C. P., et al. 2009, ApJ, 691, 1058
Davis, T. M., Mörtsell, E., Sollerman, J., et al. 2007, ApJ, 666, 716
Dvali, G., Gabadadze, G., & Porrati, M. 2000, Phys. Lett. B, 485, 208
Eisenstein, D. J., Zehavi, I., Hogg, D. W., et al. 2005, ApJ, 633, 560
Feng, B., Wang, X., & Zhang, X. 2005, Phys. Lett. B, 607, 35
Frank, V. B. & Bersini, H. 2005, Journal of Computational and Applied Mathematics, 181, 157
Freese, K. & Lewis, M. 2002, Phys. Lett. B, 540, 1
Futamase, T. & Yoshida, S. 2001, Progress of Theoretical Physics, 105, 887
Gladders, M. D., Hoekstra, H., Yee, H. K. C., Hall, P. B., & Barrientos, L. F. 2003, ApJ, 593, 48
Gorini, V., Kamenshchik, A., Moschella, U., & Pasquier, V. 2005, in The Tenth Marcel Grossmann Meeting. On recent developments in theoretical and experimental general relativity, gravitation and relativistic field theories, eds. M. Novello, S. Perez Bergliaffa, & R. Ruffini, 840
Hennawi, J. F., Gladders, M. D., Oguri, M., et al. 2008, AJ, 135, 664
Jones, M. E., Edge, A. C., Grainge, K., et al. 2005, MNRAS, 357, 518
Komatsu, E., Dunkley, J., Nolta, M. R., et al. 2009, ApJS, 180, 330
Kowalski, M., Rubin, D., Aldering, G., et al. 2008, ApJ, 686, 749
Lewis, A. & Bridle, S. 2002, Phys. Rev. D, 66, 103511
Lynds, R. & Petrosian, V. 1986, in Bulletin of the American Astronomical Society, Vol. 18, 1014
Mahdavi, A., Hoekstra, H., Babul, A., & Henry, J. P. 2008, MNRAS, 384, 1567
Majumdar, S. & Mohr, J. J. 2004, ApJ, 613, 41
Mason, B. S., Myers, S. T., & Readhead, A. C. S. 2001, ApJ, 555, L11
Milgrom, M. 2001, Acta Physica Polonica B, 32, 3613
Molnar, S. M., Haiman, Z., Birkinshaw, M., & Mushotzky, R. F. 2004, ApJ, 601, 22
Murray, S. S. & WFXT Team. 2010, in Bulletin of the American Astronomical Society, Vol. 41, Bulletin of the American Astronomical Society, 520
Navarro, J. F., Frenk, C. S., & White, S. D. M. 1996, ApJ, 462, 563
Oguri, M. & Takada, M. 2011, Phys. Rev. D, 83, 023008
Ono, T., Masai, K., & Sasaki, S. 1999, PASJ, 51, 91
Ota, N. & Mitsuda, K. 2004, A&A, 428, 757
Ota, N., Murase, K., Kitayama, T., et al. 2008, A&A, 491, 363
Paczynski, B. & Gorski, K. 1981, ApJ, 248, L101
Pen, U. 1997, New Astron., 2, 309
Perlmutter, S., Aldering, G., Goldhaber, G., et al. 1999, ApJ, 517, 565
Powell, M. J. D. 1994, in In Advances in Optimization and Numerical Analysis, Vol. 275, 51–67
Powell, M. J. D. 2002, Mathematical Programming, 92, 555
Predehl, P., Andritschke, R., Böhringer, H., et al. 2010, in Presented at the Society of Photo-Optical Instrumentation Engineers (SPIE) Conference, Vol. 7732, Society of Photo-Optical Instrumentation Engineers (SPIE) Conference Series
Press, W. H. & Schechter, P. 1974, ApJ, 187, 425
Reese, E. D., Carlstrom, J. E., Joy, M., et al. 2002, ApJ, 581, 53
Riess, A. G., Filippenko, A. V., Challis, P., et al. 1998, AJ, 116, 1009

Riess, A. G., Strolger, L.-G., Tonry, J., et al. 2004, ApJ, 607, 665
Rosati, P., Borgani, S., & Norman, C. 2002, ARA&A, 40, 539
Sand, D. J., Treu, T., Ellis, R. S., & Smith, G. P. 2005, ApJ, 627, 32
Sasaki, S. 1996, PASJ, 48, L119
Schmidt, R. W. & Allen, S. W. 2007, MNRAS, 379, 209
Schmidt, R. W., Allen, S. W., & Fabian, A. C. 2004, MNRAS, 352, 1413
Schneider, P., Ehlers, J., & Falco, E. E. 1992, Gravitational Lenses
Sereno, M. 2002, A&A, 393, 757
Sereno, M. & Longo, G. 2004, MNRAS, 354, 1255
Smith, G. P., Edge, A. C., Eke, V. R., et al. 2003, ApJ, 590, L79
Spergel, D. N., Bean, R., Doré, O., et al. 2007, ApJS, 170, 377
Spergel, D. N., Verde, L., Peiris, H. V., et al. 2003, ApJS, 148, 175
Sunyaev, R. A. & Zeldovich, Y. B. 1972, Comments on Astrophysics and Space Physics, 4, 173
Vikhlinin, A., Kravtsov, A. V., Burenin, R. A., et al. 2009, ApJ, 692, 1060
Voit, G. M. 2005, Reviews of Modern Physics, 77, 207
Walsh, D., Carswell, R. F., & Weymann, R. J. 1979, Nature, 279, 381
White, N. E., Parmar, A., Kunieda, H., et al. 2010, in American Institute of Physics Conference Series, Vol. 1248, American Institute of Physics Conference Series, eds. A. Comastri, L. Angelini, & M. Cappi, 561
White, S. D. M. & Frenk, C. S. 1991, ApJ, 379, 52
White, S. D. M., Navarro, J. F., Evrard, A. E., & Frenk, C. S. 1993, Nature, 366, 429
Yamamoto, K. & Futamase, T. 2001, Progress of Theoretical Physics, 105, 707
Zhang, H. & Zhu, Z. 2006, Phys. Rev. D, 73, 043518
Zhu, Z. & Fujimoto, M. 2004, ApJ, 602, 12
Zhu, Z., Fujimoto, M., & He, X. 2004a, A&A, 417, 833
Zhu, Z., Fujimoto, M., & He, X. 2004b, ApJ, 603, 365
Zhu, Z.-H. 2004, A&A, 423, 421